

Article

# A High-Efficient Carbon-Coated Iron-Based Fenton-Like Catalyst with Enhanced Cycle Stability and Regenerative Performance

Xin Li <sup>1</sup>, Jiankang Wang <sup>2,\*</sup>, Xiao Zhang <sup>1</sup>, Xianjin Hou <sup>1</sup>, Hongbo Xu <sup>1</sup>, Zhongping Yao <sup>1,\*</sup>  and Zhaohua Jiang <sup>1</sup>

<sup>1</sup> State Key Laboratory of Urban Water Resource and Environment, School of Chemistry and Chemical Engineering, Harbin Institute of Technology, Harbin 150001, China; 18S025131@stu.hit.edu.cn (X.L.); 19B925081@stu.hit.edu.cn (X.Z.); 19S025113@stu.hit.edu.cn (X.H.); iamxhb@hit.edu.cn (H.X.); jiangzhaohua@hit.edu.cn (Z.J.)

<sup>2</sup> College of Materials Science and Engineering, Yangtze Normal University, Chongqing 408100, China

\* Correspondence: wangjiankang@yznu.edu.cn (J.W.); yaozhongping@hit.edu.cn (Z.Y.); Tel.: +86-1573-658-4680 (J.W.); +86-1664-502-1313 (Z.Y.)

Received: 1 December 2020; Accepted: 18 December 2020; Published: 19 December 2020



**Abstract:** Carbon coated iron-based Fenton-like catalysts are now widely studied in wastewater treatment. However, their poor stability is still a big challenge and the related regenerative performance is seldom investigated. Herein, a carbon-coated Fe<sub>3</sub>O<sub>4</sub> on carbon cloth (cc/Fe<sub>3</sub>O<sub>4</sub>@C) was prepared with glucose as carbon source via electrodeposition and ethanol solvothermal methods. An amorphous carbon layer with polar C-groups covers the surface of Fe<sub>3</sub>O<sub>4</sub>, which presents a flaky cross-linked network structure on the carbon cloth (cc). The cc/Fe<sub>3</sub>O<sub>4</sub>@C exhibits an improved catalytic activity with nearly 84% phenol was removed within 35 min with polar C-groups. What's more, around 80% phenol can still be degraded in 120 min after 14 degradation cycles. After the regeneration treatment, the degradation performance was restored to the level of the fresh in the first two regenerations. The enhanced cycle stability and regeneration performance of the catalyst are as follows: Firstly, the catalyst's composition and structure were recovered; Secondly, the reduction effect of the amorphous carbon layer ensuring timely supplement of Fe<sup>2+</sup> from Fe<sup>3+</sup>. Also, the carbon layer reduces Fe leaching during the Fenton-like process.

**Keywords:** cc/Fe<sub>3</sub>O<sub>4</sub>@C Fenton-like catalyst; regeneration; ethanol solvothermal; cycle stability; phenol degradation

## 1. Introduction

The increasingly prominent issue of water pollution has become a worldwide environmental problem [1]. Advanced oxidation processes (AOP) are some of the most powerful technologies to treat organic pollutants by virtue of the potent oxidizing hydroxyl radicals (•OH) they produce [2]. Among them, researchers have favored heterogeneous Fenton catalysts due to their advantages of overcoming the strict pH requirement and reducing the Fe<sup>2+</sup> losses which occur in traditional Fenton oxidation [3,4].

Iron-based Fenton-like catalysts such as zero-valent iron (ZVI) [5], iron oxides [6,7], and surface/structure modified catalyst [8,9] have attracted more and more attention due to their easy preparation, high efficiency, and reusability [10,11]. Liang et al. [12] showed that Fe<sup>0</sup> could degrade 98% of rhodamine B (RhB) in 60 min. Xue et al. [13] revealed that the iron leaching rate was low under neutral conditions and there was no performance loss in the secondary reaction. Moreover, the structural design or surface modification can further improve the catalytic activity of the iron-based

Fenton-like catalysts [14]. The Cu/Fe mesoporous silica hollow sphere as a heterogeneous Fenton-like catalyst could remove 99% orange II (O II) within 120 min [15]. Zhong et al. [16] used Fe<sub>3</sub>O<sub>4</sub>-Mn<sub>3</sub>O<sub>4</sub> nanocomposites as a Fenton-like catalyst and removed more than 99% sulfamethazine in 50 min. Zhang's group [17] found that the rate of generating hydroxyl radicals with FeS<sub>2</sub> was 1–3 orders of magnitude greater than that of commonly used metal-doped iron-based catalysts, which also broadened the applicable range of pH value (3.2–9.2). The introduction of carbon materials, such as activated carbon [18], graphene [19,20], carbon nanotubes [21], carbon quantum dots [22] is an ideal way to optimize iron-based Fenton-like catalysts. Carbon coating can weaken the iron leaching from the catalysts, their unpaired  $\pi$  electrons can also become catalysts that react with H<sub>2</sub>O<sub>2</sub> to generate hydroxyl radicals to facilitate the catalytic process [23,24]. Besides, the reducibility of carbon material can promote the conversion of Fe<sup>3+</sup> to Fe<sup>2+</sup>, adjust the composition of catalyst, and improve the circulation stability of catalyst. [9]. Table 1 summarizes the degradation performances of various carbon-modified iron-based catalysts. Generally, most of the carbon-coated catalysts exhibit excellent degradation performance for the first cycle. Particularly, Fe@C yolk-shell has the same degradation performance after three cycles [25], while that performance of core-shell Fe<sub>3</sub>O<sub>4</sub>@C remains unchanged after five cycles [26]. However, as for most catalysts, their activity gradually declines with the number of cycle times. Given the practical application, the regeneration of the catalyst is a great strategy to improve cycle stability. However, fewer reports are focusing on the regeneration of iron-based Fenton-like catalysts.

**Table 1.** The performance of different carbon-modified iron-based catalysts.

Catalyst	Preparation	Degradable Substances	pH	Time Degradation	Cycles; Last Degradation	Ref.
Fe-AC (activated carbon)	impregnation of ferrous sulfate	Chicago Sky Blue (CSB)	3	40–50 min 88% (pH = 3)	3 88%	[18]
$\alpha$ -FeOOH@GCA	in-situ hydrolysis	Orange II (OII)	3–10	10 min 23.7%	6 6%	[19]
CoFe <sub>2</sub> O <sub>4</sub> -rGO	high temperature thermal decomposition	Acid Orange 7 (AO7)	3–9	120 min 76.9%	5 67.85%	[20]
Fe <sub>25</sub> Cu <sub>75</sub> /CNT	wetness impregnation	paracetamol	3–6.6	120 min 87.8% (pH = 3)	3 72.8%	[21]
Fe@Fe <sub>3</sub> O <sub>4</sub> /OVs@CQDs	solvothelmal electrodeposition	phenol	4–6.5	10 min 99% (pH = 4)	4 99%	[22]
Fe@C yolk-shell	hydrothermal and thermal calcination	4-chlorophenol	4	12 min 100% (pH = 4)	3 100%	[25]
core-shell Fe <sub>3</sub> O <sub>4</sub> @C	hydrothermal dehydrogenation	octane	5	60 min 83.55% (pH = 7.5)	5 83.55%	[26]
Fe <sub>3</sub> O <sub>4</sub> /SiO <sub>2</sub> /C	hydrothermal dehydrogenation	methylene blue (MB)	3.5–9.5	28 min 96% (pH = 7.5)	8 82.0%	[27]
$\gamma$ -Fe <sub>2</sub> O <sub>3</sub> /C	one-step aerosol-based procession	methylene blue (MB)	3–9	240 min 100% (pH = 7)	5 84.0%	[28]
Fe <sub>3</sub> O <sub>4</sub> @C NPs	co-precipitation hydrothermal dehydrogenation	methylene blue (MB)	3–8	120 min 99.4% (pH = 3)	4 74.3%	[29]
GO-Fe <sub>3</sub> O <sub>4</sub>	codeposition and hummer method	Acid Orange 7 (AO7)	/	/	7 98%–99%	[30]
Fe <sub>3</sub> O <sub>4</sub> /TiO <sub>2</sub> /C	hydrothermal dehydrogenation	methylene blue (MB)	4–9	140 min 82% (pH = 6)	8 >60%	[31]

One of the major factors for the attenuated catalytic activity in the cycling experiment is the limited conversion rate from Fe<sup>3+</sup> to Fe<sup>2+</sup>, which leads to the growing amount of Fe<sup>3+</sup> during the degradation process. Therefore, the process of regenerating a catalyst is the enhancing conversion

of  $\text{Fe}^{3+}$  to  $\text{Fe}^{2+}$  to a certain degree. Inspired by the reducibility of carbon materials, we proposed a regeneration strategy for carbon-modified iron-based Fenton-like catalysts through the ethanol solvothermal method. The formed carbon layer after the regeneration treatment not only prevents the iron leaching but also maintain a timely supplement of  $\text{Fe}^{2+}$  through the reduction of  $\text{Fe}^{3+}$  by the carbon layer during the catalytic process. Therefore, we prepared a carbon-coated iron oxide catalyst by a compound strategy of electrodeposition and ethanol solvothermal treatment with the glucose served as a carbon source. After a certain number of cycles, the catalyst regenerated by ethanol solvothermal treatment showed the same catalytic activity as the fresh. The degradability of the catalyst has been restored, indicating an excellent regeneration performance. This work realizes the regeneration of carbon-coated iron-based catalysts and provides a way for the regeneration of various types of catalysts.

## 2. Results and Discussion

### 2.1. Characterization of Iron Oxide Fenton-Like Catalysts

Figure 1 shows XRD patterns and the SEM images about the surface morphologies of iron oxide Fenton-like catalysts. In Figure 1a, it can be judged that the main phase of iron oxide prepared by the electrodeposition method is  $\text{Fe}_2\text{O}_3$ . However, the  $\text{Fe}_2\text{O}_3$  coated on the surface of carbon cloth is discontinuous and inhomogeneous in Figure 1c, this sample is named as  $\text{cc}/\text{Fe}_2\text{O}_3$ . Figure 1b revealed that after adding glucose to ethanol solvothermal reaction, the main phase of the carbon-coated iron oxide catalyst turns into  $\text{Fe}_3\text{O}_4$ , which is due to the reducibility of carbon produced by the decomposition of glucose [32,33].

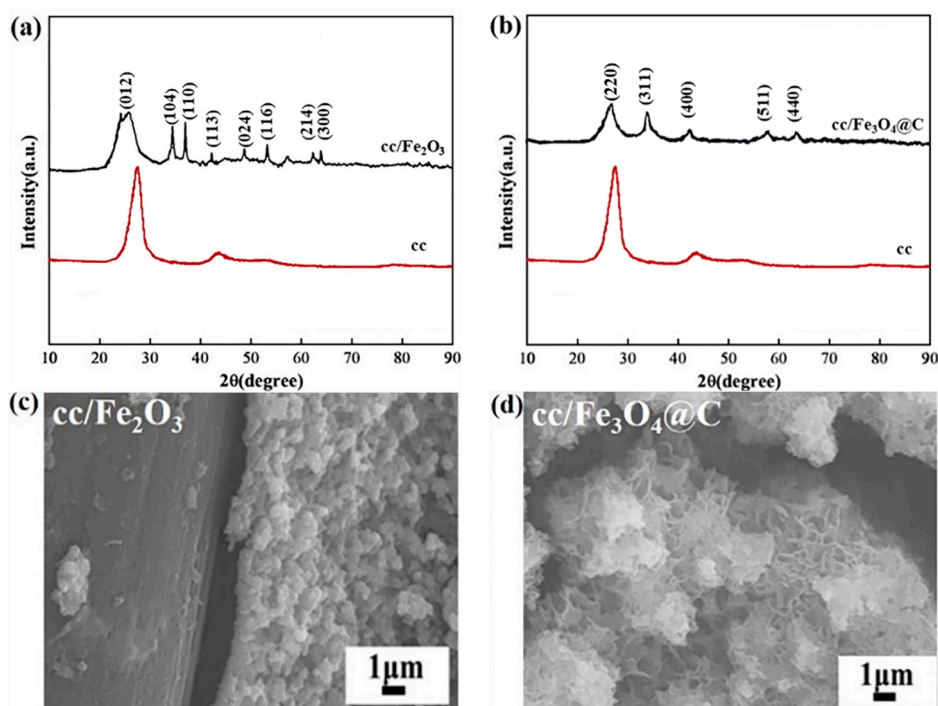


**Figure 1.** XRD patterns: (a)  $\text{cc}/\text{Fe}_2\text{O}_3$ , (b)  $\text{cc}/\text{Fe}_3\text{O}_4@\text{C}$ , and SEM images: (c)  $\text{cc}/\text{Fe}_2\text{O}_3$ , (d)  $\text{cc}/\text{Fe}_3\text{O}_4@\text{C}$ .

According to the EDS spectra (Table S1), the increased carbon content and the decreased iron content confirmed the carbon is deposited on the surface of  $\text{Fe}_3\text{O}_4$  densely (Figure 1d). As the amount of deposition increased, a carbon layer with a flaky cross-linked network structure formed, thereby the specific surface of  $\text{cc}/\text{Fe}_3\text{O}_4@\text{C}$  is expanded. The carbon layer might exist in an amorphous state, so it doesn't appear in XRD.

In order to further study the composition and the valence state of each element,  $cc/Fe_3O_4@C$  was analyzed by XPS, with the results shown in Figure 2. It can be seen from Figure 2a that the  $cc/Fe_3O_4@C$  is mainly composed of three elements: C, O, and Fe, which is consistent with the EDS result in Table S1. In Fe 2p XPS spectrum (Figure 2b), Fe 2p<sub>1/2</sub> and Fe 2p<sub>3/2</sub> peaks are clearly presented. The Fe 2p<sub>3/2</sub> peak is divided into 709.4 eV (Fe<sup>2+</sup>) and 710.8 eV (Fe<sup>3+</sup>), 713.7 eV and 722.7 eV are corresponded to Fe<sup>2+</sup> and Fe<sup>3+</sup> of Fe 2p<sub>1/2</sub> peak, separately [34]. Figure 2c is the O1s spectrum, which can be fitted into six characteristic peaks: 529.2 eV, 529.7 eV, 530.3 eV, 530.9 eV, 531.6 eV, and 532.4 eV, attributed to the electronic binding energy of O-H, O-Fe (Fe<sup>3+</sup>), O-Fe (Fe<sup>2+</sup>), C-O, C=O, in turn [30]. In addition, the C 1s XPS spectrum (Figure 2d) indicates that carbon atoms are in the chemical stages of C-OH (285.2 eV), C=O (286.6 eV), COO<sup>-</sup> (288.6 eV), sp<sup>2</sup>C (284.4 eV), and sp<sup>3</sup>C (284.7 eV) [35], these polar C-groups were derived from the thermal decomposition of ethanol and glucose. The sp<sup>2</sup>C and sp<sup>3</sup>C belonged to the carbon cloth.

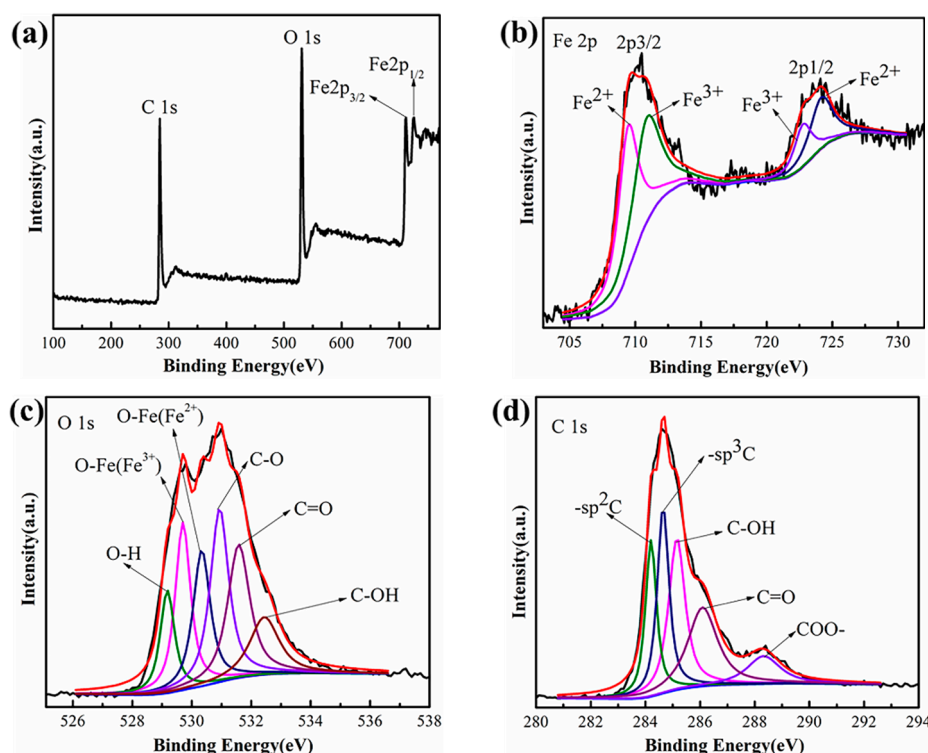


**Figure 2.** XPS spectrums of  $cc/Fe_3O_4@C$ : (a) Full spectrum; (b) Fe 2p; (c) O 1s; (d) C 1s.

In all,  $cc/Fe_2O_3$  was obtained through electrodeposition. After ethanol solvothermal treatment,  $cc/Fe_3O_4@C$  was produced successfully with an amorphous carbon layer coated on it. Its flaky cross-linked network structure contributes to the enlarged specific surface area, and the polar C-groups on the carbon layer strengthen the ability to adsorb phenol and H<sub>2</sub>O<sub>2</sub>. Therefore, the prepared  $cc/Fe_3O_4@C$  is expected to ensure a better degradation performance.

## 2.2. Degradation Performance of Iron Oxide Fenton-Like Catalysts

The degradation test of phenol evaluated the catalytic activities of  $cc/Fe_2O_3$  and  $cc/Fe_3O_4@C$ . Figure 3 presents the degradation curves and kinetic curves of  $cc/Fe_2O_3$  and  $cc/Fe_3O_4@C$ . When H<sub>2</sub>O<sub>2</sub> or catalyst is added to the system alone, the phenol concentration hardly changes with time, and almost no degradation occurs. When  $cc/Fe_2O_3$  and H<sub>2</sub>O<sub>2</sub> are added simultaneously, it takes 80 min to degrade 80% phenol. While, in the system of  $cc/Fe_3O_4@C$  and H<sub>2</sub>O<sub>2</sub>, the degradation time can be significantly shortened. It takes 40 min to eliminate 84.3% phenol. In Figure 3b, phenol's degradation by different iron oxide Fenton-like systems corresponds to the first-order kinetic curve. The kinetic parameter

of  $cc/Fe_2O_3$  is 0.0219, and that of  $cc/Fe_3O_4@C$  is extended to 0.0498. After degradation, phenol is oxidized to hydroquinone, benzoquinone, et al., firstly. After that, some intermediates such as maleic acid, oxalic acid, succinic acid, acetic acid, and formic acid are formed by ring opening. Finally, it is completely degraded to  $CO_2$  and  $H_2O$  [36–38]. In the  $cc/Fe_3O_4@C$  system, the TOC of phenol solution at different reaction times was measured with the result shown in Figure S1. The removal rate of the TOC is 32.77% in 30 min, and up to 40.41% when the reaction time is prolonged to 40 min.

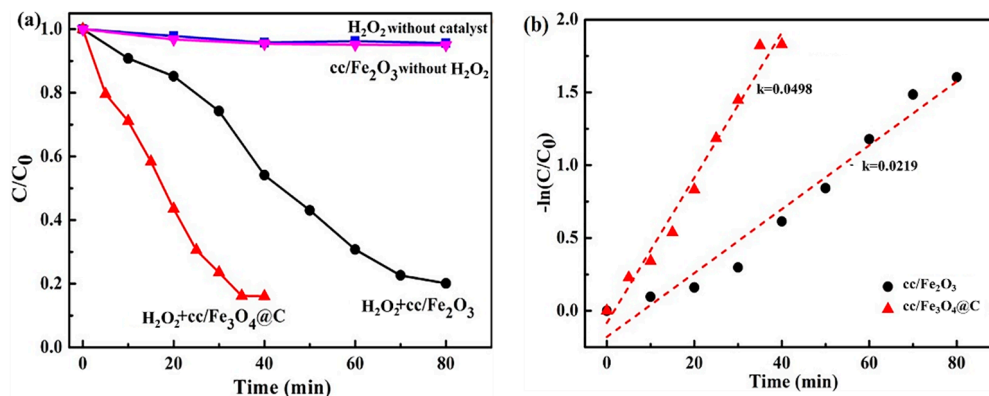


**Figure 3.** (a) Phenol degradation by different systems, (b) the kinetic curves of Fenton-like degradation of phenol by  $cc/Fe_2O_3$  and  $cc/Fe_3O_4@C$ . Experimental conditions: 35 ppm phenol, 6 mmol  $H_2O_2$ , pH = 4.

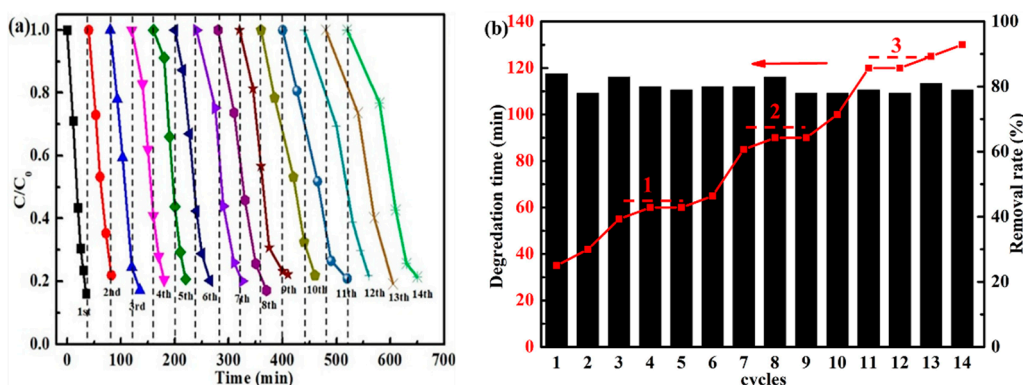
Generally,  $Fe_3O_4$  has more catalytic activity than  $Fe_2O_3$ , and the carbon layer can reduce the produced  $Fe^{3+}$  to  $Fe^{2+}$  during degradation to immediately supplement the  $Fe^{2+}$  in the system. Therefore, the catalyst exhibits higher catalytic activity and stability. In addition, the carbon layer with polar C-groups can adsorb more phenol and  $H_2O_2$ , and its flaky cross-linked network structure expands the specific surface area of the catalyst [39]. It also helps to improve catalytic degradation performance further.

Figure S2 illustrates the total iron dissolution of the two different systems, the iron dissolution of  $cc/Fe_2O_3$  is 2.76 ppm. After carbon coating with ethanol solvothermal ( $cc/Fe_3O_4@C$ ), it is reduced to 0.83 ppm. The coated carbon layer can not only change the phase composition of the catalyst but also lessen iron dissolving from the inside to improve the stability of the catalyst. Under this condition we studied the evolution of 6 mmol  $H_2O_2$  with time, the result is shown in Figure S3. The content of  $H_2O_2$  in the system decreased gradually, in the first 40 min, 65%  $H_2O_2$  in the system is consumed. Subsequently, the content of  $H_2O_2$  is hardly changed until 80 min. Therefore, the concentration of  $H_2O_2$  remains a proper level during the Fenton-like process.

### 2.3. Cyclic Stability of Iron Oxide Fenton-Like Catalyst

In Fenton reactions, cycle stability is also an essential factor. In Figure S2, the cycle stability of  $cc/Fe_2O_3$  is inferior and still less than 10% after 360 min in the second cycle. Without the protection of the carbon layer, the  $Fe_2O_3$  is easy to leach during the first phenol degradation process, which can be verified by the surface morphologies of  $cc/Fe_2O_3$  before and after phenol degradation (Figure S4).

However,  $cc/Fe_3O_4@C$  shows superior cycle stability. The catalyst was cyclically tested when phenol's degradation rate reaches about 80% each time, and the results are shown in Figure 4. Figure 4a is the degradation curves of  $cc/Fe_3O_4@C$ , Figure 4b is the statistics of degradation time and removal rate of each degradation. With the addition of the cycles, the time required for each process gradually extends, which increases linearly in the first three cycles. The degradation time can be roughly divided into three platforms: it grows to 60 min from the 3rd to the 6th cycles, 90–100 min is required for the 7th to 10th degradations, when the number of cycles is 11 or more, it takes over 120 min to remove around 80% phenol.



**Figure 4.** (a) cyclic stability of cc/Fe<sub>3</sub>O<sub>4</sub>@C to activate H<sub>2</sub>O<sub>2</sub> for phenol degradation, (b) degradation time for each cycle and corresponding phenol removal efficiency. Experimental conditions: 35 ppm phenol, 6 mmol H<sub>2</sub>O<sub>2</sub>, pH = 4.

The change of catalyst cycle stability is closely related to the shift of catalyst composition and morphology. The surface morphologies of cc/Fe<sub>3</sub>O<sub>4</sub>@C before and after 14 cycles of phenol degradation can be clearly seen in SEM images (Figure 5). The flaky cross-linked network structure on the surface can still be observed, but the surface seems to be polished. This result indicates that the carbon layer is lost during the repeated tests, which will weaken the generation rate of Fe<sup>2+</sup> from Fe<sup>3+</sup> and enhance the iron dissolution. In the meantime, the decrease of active groups attached to the carbon layer will reduce the adsorption capacity. Consequently, the time required for degradation will be prolonged with the increasing number of cycles. It seems that the three platforms in Figure 4b may be related to the consumption of the carbon layer, which contributes to the results that the Fe<sup>2+</sup> is unable to be replenished timely and the total iron dissolution is enhanced.

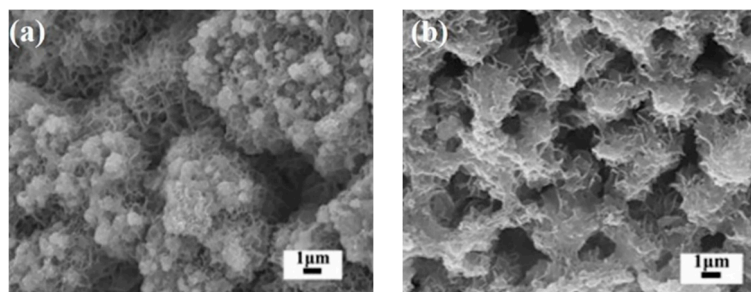


**Figure 5.** SEM images of cc/Fe<sub>3</sub>O<sub>4</sub>@C: (a) before phenol degradation (fresh), (b) after 14 cycles of phenol degradation. Experimental conditions: 35 ppm phenol, 6 mmol H<sub>2</sub>O<sub>2</sub>, pH = 4.

#### 2.4. Renewability of Iron Oxide Fenton-Like Catalyst

Combined with the result analysis of 3.3, it can be seen that the decline of catalyst degradation performance is related to the loss of carbon layer, which in turn causes iron dissolution and the attenuation in the activity of the catalyst. Therefore, the carbon layer coating by ethanol solvothermal treatment should be an effective method to obtain a robust catalyst. The fresh cc/Fe<sub>3</sub>O<sub>4</sub>@C had undergone four regeneration treatments in total, and the obtained catalyst was subjected to a cycle stability test after each regeneration. When more than 80% of phenol was degraded each cycle, the next cyclic test was carried out. The specific test results are shown in Figure 6. Fresh CC/Fe<sub>3</sub>O<sub>4</sub>@C is recycled for seven times phenol degradation, at the 7th degradation, the time required for 80% degradation is extended to 80 min. Then, the first carbonization was carried out. Similarly, 35 ppm phenol is cycle degraded for 7 times, the degradation performance and cycle stability are restored. The above operations were repeated for 4 times carbonizations, consecutively. After each carbonization,

the cyclic stability of the material decreases slightly, but the first degradation rate in each cycle is almost the same.

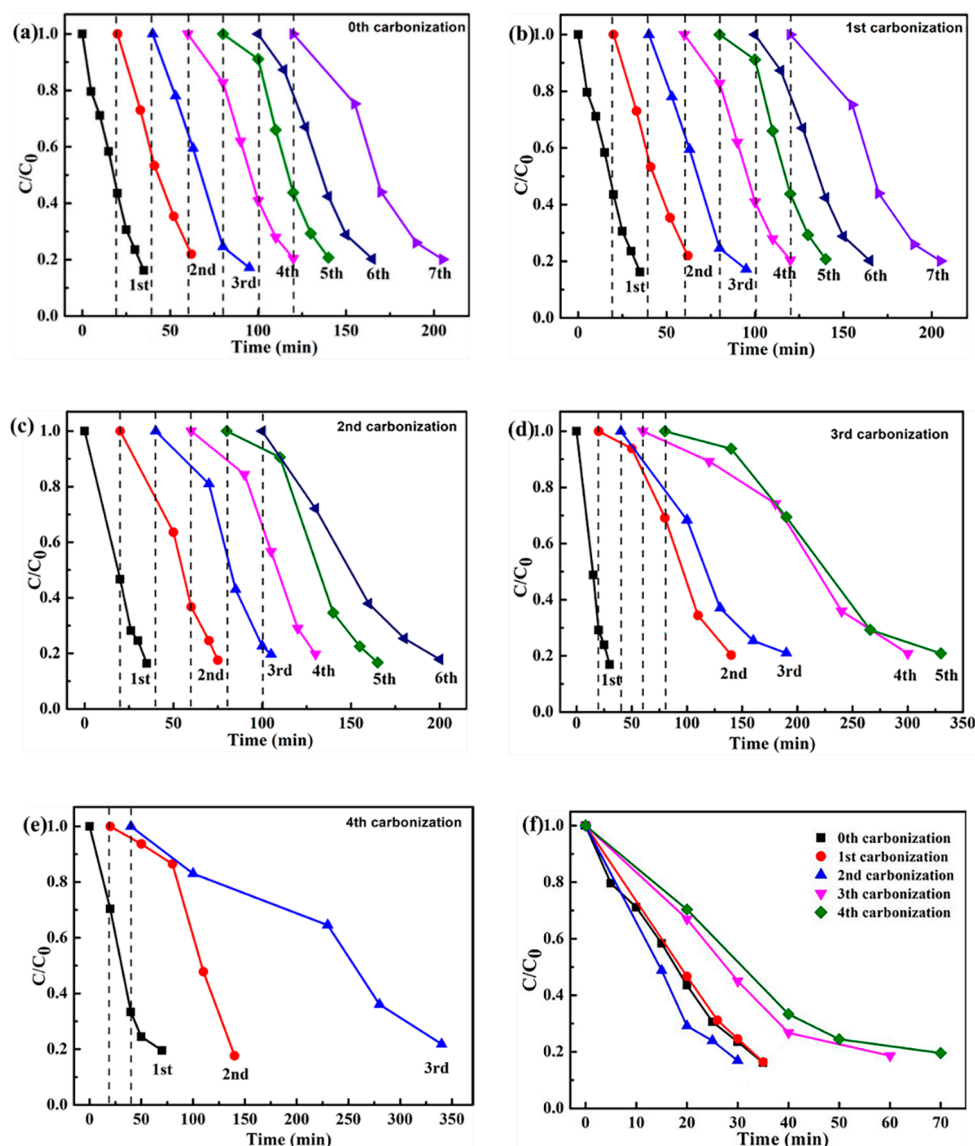


**Figure 6.** Cyclic stability of the regenerated  $cc/Fe_3O_4@C$  with different carbonization times to activate  $H_2O_2$  for phenol degradation: (a) 0th carbonization ( $cc/Fe_3O_4@C$ ); (b) 1st carbonization; (c) 2nd carbonization; (d) 3rd carbonization; (e) 4th carbonization; (f) the performance comparison of the first phenol degradation derived from the cyclic test of the regenerated  $cc/Fe_3O_4@C$ . Experimental conditions: 35 ppm phenol, 6 mmol  $H_2O_2$ , pH = 4.

Figure 7 is the first and last degradation kinetic curves of the fresh and the re-carbon coated  $cc/Fe_3O_4@Cs$ . The kinetic constant of the fresh  $cc/Fe_3O_4@C$  is  $0.0505 \text{ min}^{-1}$  for the first time. In the seventh cycle, the degradation time increased to 80 min and the kinetic constant decreased to  $0.0044 \text{ min}^{-1}$ . After that, the first regeneration treatment was carried out, 83.6% phenol is degraded in 40 min, the kinetic constant goes back to  $0.0516 \text{ min}^{-1}$ , and the cycle stability is still favorable.

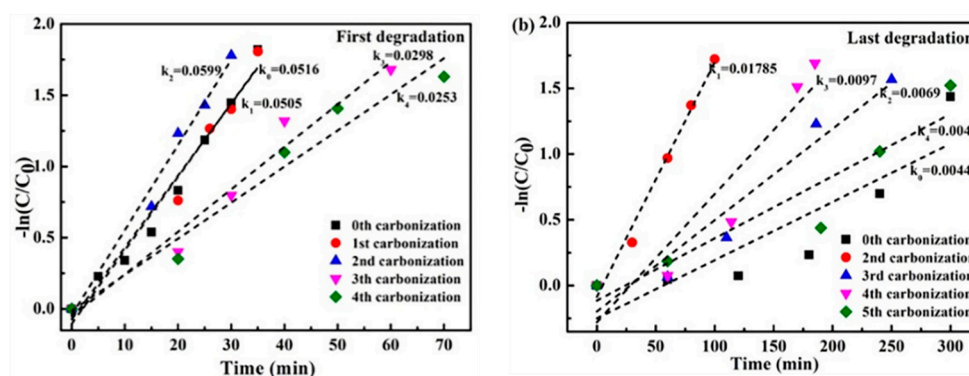


**Figure 7.** The kinetic curves of Fenton-like degradation of phenol by the regenerated  $cc/Fe_3O_4@C$  with different carbonization times. (a) the first degradation; (b) the last degradation, Experimental conditions: 35 ppm phenol, 6 mmol  $H_2O_2$ , pH = 4.

According to Figures 6f and 7a, after the first two carbonizations, the first cycle's degradation performance can be restored to the previous level. As for the third and fourth regenerations, the degradation time required for the first cycle is extended. The kinetic parameters dropped to half of the fresh  $cc/Fe_3O_4@C$  system, and the related cycle stability is also decreased. Ethanol solvothermal treatment can indeed achieve catalyst regeneration. Still, after multiple regenerations, the catalytic performance is significantly reduced, which is associated with the decrease of iron oxide catalyst, which happens in numerous regenerations and cycle tests.

To clarify the reproducibility of  $cc/Fe_3O_4@C$ , XPS was used to analyze the composition of the degraded and regenerated  $cc/Fe_3O_4@C$ . Figure 8 is the Fe 2p<sub>3/2</sub> spectra and C1s spectra. The iron element exists as  $Fe^{2+}$  (710.4 eV) and  $Fe^{3+}$  (711.7 eV), and the ratio between them is 60:40 before the degradation. After the 7th degradation, the ratio of  $Fe^{2+}$  and  $Fe^{3+}$  decreases to 41:59, which corresponds to the decrease of catalytic activity and the prolonged degradation time. By subjecting the catalyst to the first regeneration treatment, the catalyst's proportion of  $Fe^{2+}$  in the catalyst comes back to 61%. When measured by the amount of  $Fe^{2+}$ , it can be considered that the catalytic activity can be restored to the equivalent level. Amorphous carbon can be obtained with glucose as a carbon source by a high-temperature solvothermal method, which can exert a reducing effect to convert  $Fe^{3+}$  to  $Fe^{2+}$  and thereby ensure the stability of  $cc/Fe_3O_4@C$ .

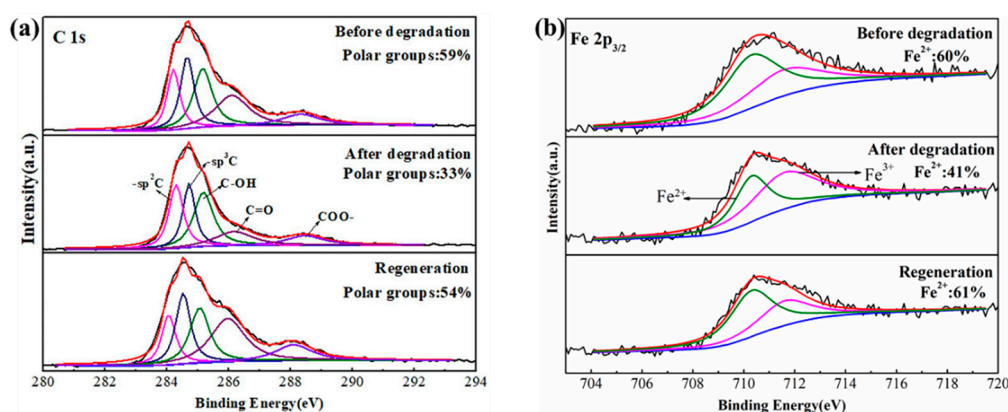


**Figure 8.** The high-resolution (a) C 1s and (b) Fe 2p XPS spectra of the fresh, the used and regenerated  $cc/Fe_3O_4@C$ .

### 3. Experimental

#### 3.1. Preparation of Carbon-Coated Iron Oxide Fenton-Like Catalyst

The iron-based catalyst was prepared by electrochemical deposition through a three-electrode system, among which carbon cloth served as the working electrode. Simultaneously, Pt foil and Ag/AgCl were the counter electrode and reference electrode, respectively. Ferric nitrate solution (0.12 mol/L) was regarded as the electrolyte to provide the iron. After electrodepositing 20 min, the carbon cloth covered with iron oxide was rinsed repeatedly in deionized water and dried in air.

Carbon-coated iron oxide catalyst was prepared via ethanol solvothermal method with glucose as carbon source. 2 cm<sup>2</sup> iron oxide catalyst supported by carbon cloth, 0.5 g glucose, and 40 mL solvent (volume ratio of ethanol and deionized water is 7:1) were added into the PTFE liner in turn, the reaction was carried at 160 °C for 12 h. And then, the sample was cooled to room temperature, rinsed repeatedly, and dried in air. In the regeneration experiments, the operation of each carbonization treatment was the same as above.

#### 3.2. Characterization Methods

The phase composition of carbon-coated iron oxide Fenton-like catalysts was detected and analyzed by X-ray diffraction (XRD, Cu K $\alpha$ ,  $\lambda = 0.15406$  nm, Rigaku D/max- $\gamma$ B diffractometer, Tokyo, Japan). The samples' surface morphologies were determined by scanning electron microscopy (Helios Nano Lab 600i SEM, Hillsboro, OR, America). X-ray photoelectron spectroscopy (XPS, Al K $\alpha$  radiation at 1486.6 eV) was used to determine the chemical composition, valence state, and content of elements on the sample surface (PHI 5400 ESCA, Waltham, MA, America).

#### 3.3. Catalytic Performance Test

The degradation experiment was carried out at  $T = 303$  K, the pH of the phenol solution (35 ppm) was adjusted to 4 with H<sub>2</sub>SO<sub>4</sub> before degradation. The catalyst and 6.0 mmol/L H<sub>2</sub>O<sub>2</sub> were immersed in the phenol solution in turn for degradation. The phenol concentration was measured with 4-aminoantipyrine at 510 nm on a UV/Vis spectrophotometer (Lambda XLS, PerkinElmer, Waltham, MA, America). And the concentrations of total irons leaching from the catalysts was evaluated by the 1,10-phenanthroline method. Total organic carbon (TOC) values were obtained using an Multi NIC 3100 total organic carbon analyzer (Analytik Jena, Jena, Germany) when the degradation of phenol degradation was 30 min and 40 min, respectively. H<sub>2</sub>O<sub>2</sub> concentration was determined by adding 1 mL of a 0.5 M H<sub>2</sub>SO<sub>4</sub> solution and 0.1 mL of TiO(SO<sub>4</sub>) (15 wt. % in diluted H<sub>2</sub>SO<sub>4</sub>) to 1 mL of the liquid sample and measuring the respective absorbance at 405 nm by UV-Vis spectrophotometer (V-560, JASCO, Tokyo, Japan).

To measure the catalyst's cyclic stability, it was washed after each degradation with deionized water, and then the degradation test was repeated under the same conditions. After repeating a certain number of tests, the catalyst was regenerated through the ethanol solvothermal method. The regeneration performance was evaluated by the time required for the degradation rate around 80 % in each degradation process.

### 4. Conclusions

In summary, an amorphous carbon-coated iron oxide Fenton-like catalyst was synthesized successfully on a carbon cloth through a two-step method of electrodeposition and ethanol solvothermal treatment. The catalyst's composition and structure, catalytic activities and regenerated performance have been investigated, and the following conclusions are drawn as follows:

- (1) Glucose works as a carbon source during the ethanol solvothermal treatment, which both transforms Fe<sub>2</sub>O<sub>3</sub> into Fe<sub>3</sub>O<sub>4</sub> through reduction effect, and coats on Fe<sub>3</sub>O<sub>4</sub> in a flaky cross-linked network structure with polar C-groups.

- (2) The cc/Fe<sub>3</sub>O<sub>4</sub>@C shows excellent catalytic activities, the removal rate of 35 ppm phenol reaches 84% within 35 min when H<sub>2</sub>O<sub>2</sub> is 6 mmol and pH is 4. The degradation process corresponds to the first-order kinetic curve ( $k = 0.0498 \text{ min}^{-1}$ ). The catalysts present the enhanced cycle stability. Although the degradation time is prolonged to 120 min, the removal rate is still around 80 % in the 14th cycle.
- (3) Ethanol solvothermal treatment with glucose as carbon source for the used catalysts can realize the regeneration. The kinetic constants of the first two regenerated catalysts are consistent with that of the fresh one. However, the last two regenerations' constant is lowered to half of the original, which may originate from the inevitable iron oxide loss.
- (4) The formation of the amorphous carbon layer on catalysts' surface determines the enhanced cycle stability and regenerative performance. The carbon layer makes the consumed Fe<sup>2+</sup> replenished in time by reducing the Fe<sup>3+</sup> while cutting back the iron leaching. Besides, polar C-groups of the carbon layer are conducive to the adsorption of phenol and H<sub>2</sub>O<sub>2</sub>, further promoting the catalyst's degradation performance.

**Supplementary Materials:** The following are available online at <http://www.mdpi.com/2073-4344/10/12/1486/s1>, Figure S1: Total iron dissolution of cc/Fe<sub>2</sub>O<sub>3</sub> and cc/Fe<sub>3</sub>O<sub>4</sub>@C, Figure S2: Cyclic stability of cc/Fe<sub>2</sub>O<sub>3</sub>, Figure S2: SEM image of cc/Fe<sub>2</sub>O<sub>3</sub>: (a) before degradation, (b) after 1st degradation, Table S1: EDS of iron oxide catalyst before and after carbon-coated.

**Author Contributions:** Conception, Z.Y., J.W. and Z.J.; Design, Z.Y. and X.L.; Experiment and data processing, X.H. and X.L.; Writing, X.L.; Review manuscript, Z.Y., J.W., H.X., and X.Z. All authors have read and agreed to the published version of the manuscript.

**Funding:** This work is supported by National Natural Science Foundation of China (No. 51571076, 21906008), Open project of State Key Laboratory of Urban Water Resource and Environment of Harbin Institute of Technology (No. HCK201716), Chongqing Basic and Frontier Research Program (cstc2018jcyjAX0774) and Science and Technology Research Program of Chongqing Municipal Education Commission (No. KJQN201901420).

**Conflicts of Interest:** The authors declare that they have no known competing financial interests or personal relationships that could have appeared to influence the work reported in this paper.

## References

1. Gou, N.; Yuan, S.; Lan, J.; Gao, C.; Alshwabkeh, A.N.; Gu, A.Z. A Quantitative Toxic Genomics Assay Reveals the Evolution and Nature of Toxicity during the Transformation of Environmental Pollutants. *Environ. Sci. Technol.* **2014**, *48*, 8855–8863. [[CrossRef](#)]
2. Moreira, F.C.; Boaventura, R.A.R.; Brillas, E.; Vitor, J.P.V. Electrochemical advanced oxidation processes: A review on their application to synthetic and real wastewaters. *Appl. Catal. B Environ.* **2017**, *202*, 217–261. [[CrossRef](#)]
3. Wang, J.L.; Xu, L.J. Advanced Oxidation Processes for Wastewater Treatment: Formation of Hydroxyl Radical and Application. *Crit. Rev. Environ. Sci. Technol.* **2012**, *42*, 251–325. [[CrossRef](#)]
4. Zepp, R.G.; Faust, B.C.; Holgne, J. Hydroxyl radical formation in aqueous reactions (pH 3–8) of iron(II) with hydrogen peroxide: The Photo-Fenton reaction. *Environ. Sci. Technol.* **1992**, *26*, 313–319. [[CrossRef](#)]
5. Chen, Y.P.; Li, M.Y.; Chen, P.J.; Zheng, Y.M. Electrospun spongy zero-valent iron as excellent electro-Fenton catalyst for enhanced sulfathiazole removal by a combination of adsorption and electro-catalytic oxidation. *J. Hazard. Mater.* **2019**, *371*, 576–585. [[CrossRef](#)] [[PubMed](#)]
6. He, J.; Yang, X.; Men, B.; Wang, D. Interfacial mechanisms of heterogeneous Fenton reactions catalyzed by iron-based materials: A review. *J. Environ. Sci.* **2016**, *1*, 97–109. [[CrossRef](#)] [[PubMed](#)]
7. Rusevova, K.; Kopinke, F.D.; Georgi, A. Nano-sized magnetic iron oxides as catalysts for heterogeneous Fenton-like reactions-Influence of Fe (II)/Fe (III) ratio on catalytic performance. *J. Hazard. Mater.* **2012**, *241–242*, 433–440. [[CrossRef](#)] [[PubMed](#)]
8. Ghasemi, H.; Aghabarari, B.; Alizadeh, M.; Khanlarkhani, A.; Abu-Zahra, N. High efficiency decolorization of wastewater by Fenton catalyst: Magnetic iron-copper hybrid oxides. *J. Water Process. Eng.* **2020**, *37*, 101540. [[CrossRef](#)]

9. Yamaguchi, R.; Kurosu, S.; Suzuki, M.; Kawase, Y. Hydroxyl radical generation by zero-valent iron/Cu (ZVI/Cu) bimetallic catalyst in wastewater treatment: Heterogeneous Fenton/Fenton-like reactions by Fenton reagents formed in-situ under oxic conditions. *Chem. Eng. J.* **2018**, *334*, 1537–1549. [[CrossRef](#)]
10. Nidheesh, P.V. Heterogeneous Fenton catalysts for the abatement of organic pollutants from aqueous solution: A review. *RSC Adv.* **2015**, *5*, 40552–40577. [[CrossRef](#)]
11. Hartmann, M.; Kullmann, S.; Keller, H. Wastewater Treatment with Heterogeneous Fenton-type Catalysts Based on Porous Materials. *J. Mater. Chem.* **2010**, *20*, 9002–9017. [[CrossRef](#)]
12. Liang, L.; Cheng, L.; Zhang, Y.; Wang, Q.; Meng, X. Efficiency and mechanisms of rhodamine B degradation in Fenton-like systems based on zero-valent iron. *RSC Adv.* **2020**, *10*, 28509–28515. [[CrossRef](#)]
13. Xue, X.; Hanna, K.; Deng, N. Fenton-like oxidation of Rhodamine B in the presence of two types of iron (II, III) oxide. *J. Hazard. Mater.* **2009**, *166*, 407–414. [[CrossRef](#)] [[PubMed](#)]
14. Wei, G.; Liang, X.; He, Z.; Liao, Y.; Xie, Z.; Liu, P.; Ji, S.; He, H.; Li, D.; Zhang, J. Heterogeneous activation of Oxone by substituted magnetites  $Fe_{3-x}M_xO_4$  (Cr, Mn, Co, Ni) for degradation of Acid Orange II at neutral pH. *J. Mol. Catal. A Chem.* **2015**, *398*, 86–94. [[CrossRef](#)]
15. Wang, J.; Liu, C.; Hussain, I.; Li, C.; Li, J.; Sun, X.; Shen, Z.; Han, W.; Wang, L. Iron-copper bimetallic nanoparticles supported on hollow mesoporous silica sphere: The effect of Fe/Cu ratio on heterogeneous Fenton degradation of dye. *RSC Adv.* **2016**, *59*, 54623–54635. [[CrossRef](#)]
16. Wan, Z.; Wang, J. Degradation of sulfamethazine antibiotics using  $Fe_3O_4$ - $Mn_3O_4$  nanocomposite as a Fenton-like catalyst. *J. Chem. Technol. Biotechnol.* **2017**, *92*, 874–883. [[CrossRef](#)]
17. Liu, W.; Wang, Y.; Ai, Z.; Zhang, L. Hydrothermal synthesis of FeS<sub>2</sub> as a high-efficiency Fenton reagent to degrade alachlor via superoxide-mediated Fe(II)/Fe(III) cycle. *ACS Appl. Mater. Interfaces* **2015**, *7*, 28534–28544. [[CrossRef](#)]
18. Mesquita, I.; Matos, L.C.; Duarte, F.; Maldonado-Hodar, F.J.; Mendes, A.; Madeira, L.M. Treatment of azo dye-containing wastewater by a Fenton-like process in a continuous packed-bed reactor filled with activated carbon. *J. Hazard. Mater.* **2012**, *237*, 30–37. [[CrossRef](#)]
19. Liu, Y.; Liu, X.; Zhao, Y.; Dionysiou, D.D. Aligned  $\alpha$ -FeOOH nanorods anchored on a graphene oxide-carbon nanotubes aerogel can serve as an effective Fenton-like oxidation catalyst. *Appl. Catal. B Environ.* **2017**, *23*, 74–86. [[CrossRef](#)]
20. Hassani, A.; Çelikdağ, G.; Eghbali, P.; Sevim, M.; Karaca, S.; Metin, Ö. Heterogeneous sono-Fenton-like process using magnetic cobalt ferrite-reduced graphene oxide ( $CoFe_2O_4$ -rGO) nanocomposite for the removal of organic dyes from aqueous solution. *Ultrason. Sonochem.* **2018**, *40*, 841–852. [[CrossRef](#)]
21. Barrios-Bermúdez, N.; González-Avendaño, M.; Lado-Touriño, I.; Cerpa-Naranjo, A.; Rojas-Cervantes, M.L. Fe-Cu Doped Multiwalled Carbon Nanotubes for Fenton-like Degradation of Paracetamol Under Mild Conditions. *Nanomaterials* **2020**, *10*, 749. [[CrossRef](#)] [[PubMed](#)]
22. Xia, Q.; Yao, Z.; Zhang, D.; Li, D.; Zhang, Z.; Jiang, Z. Rational synthesis of micronano dendritic ZVI@ $Fe_3O_4$  modified with carbon quantum dots and oxygen vacancies for accelerating Fenton-like oxidation. *J. Sci. Total Environ.* **2019**, *671*, 1056–1065. [[CrossRef](#)]
23. Dhakshinamoorthy, A.; Navalon, S.; Alvaro, M.; Garcia, H. Metal nanoparticles as heterogeneous Fenton catalysts. *ChemSusChem* **2020**, *5*, 46–64. [[CrossRef](#)] [[PubMed](#)]
24. Ramirez, J.H.; Maldonado-Hódar, F.J.; Pérez-Cadenas, A.F.; Moreno-Castilla, C.; Costa, C.A.; Madeira, L.M. Azo-dye Orange II degradation by heterogeneous Fenton-like reaction using carbon-Fe catalysts. *Appl. Catal. B Environ.* **2007**, *75*, 312–323. [[CrossRef](#)]
25. Li, X.; Gai, F.; Guan, B.; Zhang, Y.; Liu, Y.; Huo, Q. Fe@C core-shell and Fe@C yolk-shell particles for effective removal of 4-chlorophenol. *J. Mater. Chem. A* **2015**, *3*, 3988–3994.
26. Zhuang, Y.; Liu, J.; Yuan, S.; Ge, B.; Zhang, Y. Degradation of octane using an efficient and stable core-shell  $Fe_3O_4$ @C during Fenton processes: Enhanced mass transfer, adsorption and catalysis. *Appl. Surf. Sci.* **2020**, *515*, 146083. [[CrossRef](#)]
27. Wang, R.; Liu, X.; Wu, R.; Yu, B.; Li, H.; Zhang, X.; Xie, J.; Yang, S.  $Fe_3O_4/SiO_2/C$  nanocomposite as a high-performance Fenton-like catalyst in a neutral environment. *RSC Adv.* **2016**, *10*, 1039.
28. Zhan, J.; Li, M.; Zhang, X.; An, Y.; Zhou, H. Aerosol-assisted submicron  $\gamma$ - $Fe_2O_3/C$  spheres as a promising heterogeneous Fenton-like catalyst for soil and groundwater remediation: Transport, adsorption and catalytic ability. *Chin. Chem. Lett.* **2020**, *31*, 147–152. [[CrossRef](#)]

29. Zhang, X.; He, M.; Liu, J.H.; Liao, R.; Zhao, L.; Xie, J.; Wang, R.; Yang, S.; Wang, H.; Liu, Y. Fe<sub>3</sub>O<sub>4</sub>@C nanoparticles as high-performance Fenton-like catalyst for dye decoloration. *Chin. Sci. Bull.* **2014**, *59*, 3406–3412. [[CrossRef](#)]
30. Zubir, N.A.; Yacou, C.; Motuzas, J.; Zhang, X.; Zhao, X.; da Costa, J.C.D. The sacrificial role of graphene oxide in stabilising a Fenton-like catalyst GO-Fe<sub>3</sub>O<sub>4</sub>. *Chem. Commun.* **2015**, *51*, 9291–9293. [[CrossRef](#)]
31. Liu, X.; Zhang, Q.; Yu, B.; Wu, R.; Mai, J.; Wang, R.; Chen, L.; Yang, S. Preparation of Fe<sub>3</sub>O<sub>4</sub>/TiO<sub>2</sub>/C nanocomposites and their application in Fenton-like catalysis for dye decoloration. *Catalysts* **2016**, *6*, 146. [[CrossRef](#)]
32. Bohn, C.D.; Cleeton, J.P.; Müller, C.R.; Davidson, J.F.; Hayhurst, A.N.; Scott, S.A.; Dennis, J.S. The kinetics of the reduction of iron oxide by carbon monoxide mixed with carbon dioxide. *AIChE J.* **2010**, *56*, 1016–1029. [[CrossRef](#)]
33. Li, J.; Li, B.W.; Zhang, B.W. Microwave carbothermic reduction from Fe<sub>2</sub>O<sub>3</sub> to Fe<sub>3</sub>O<sub>4</sub> powders. *J. Univ. Sci. Technol. B.* **2011**, *33*, 1127–1132.
34. Jiang, Y.; Yu, Z.; Xia, Q.; Zhang, Y.; Wu, Z.; Jiang, Z.; Yao, Z.; Wu, Z. Structure and corrosion resistance of PEO ceramic coatings on AZ91D Mg alloy under three kinds of power modes. *Int. J. Appl. Ceram. Technol.* **2013**, *10*, E310–E317. [[CrossRef](#)]
35. Guo, L.; Chen, F.; Fan, X.; Cai, W.; Zhang, J. S-doped α-Fe<sub>2</sub>O<sub>3</sub> as a highly active heterogeneous Fenton-like catalyst towards the degradation of acid orange 7 and phenol. *Appl. Catal. B Environ.* **2010**, *96*, 162–168. [[CrossRef](#)]
36. Zazo, J.A.; Casas, J.A.; Mohedano, A.F.; Gilarranz, M.A.; Rodríguez, J.J. Chemical pathway and kinetics of phenol oxidation by Fenton's reagent. *Environ. Sci. Technol.* **2005**, *39*, 9295–9302. [[CrossRef](#)]
37. Wei, X.; Wu, H.; He, G.; Guan, Y. Efficient degradation of phenol using iron-montmorillonite as a fenton catalyst: Importance of visible light irradiation and intermediates. *J. Hazard. Mater.* **2017**, *321*, 408–416. [[CrossRef](#)] [[PubMed](#)]
38. Bremner, D.H.; Burgess, A.E.; Houlemare, D.; Namkung, K.C. Phenol degradation using hydroxyl radicals generated from zero-valent iron and hydrogen peroxide. *Appl. Catal. B Environ.* **2006**, *63*, 15–19. [[CrossRef](#)]
39. Fan, Z.; Kai, W.; Yan, J.; Wei, T.; Zhi, L.; Feng, J.; Ren, Y.; Song, L.; Fei, W. Facile synthesis of graphene nanosheets via Fe reduction of exfoliated graphite oxide. *ACS Nano* **2010**, *5*, 191–198. [[CrossRef](#)]

**Publisher's Note:** MDPI stays neutral with regard to jurisdictional claims in published maps and institutional affiliations.



© 2020 by the authors. Licensee MDPI, Basel, Switzerland. This article is an open access article distributed under the terms and conditions of the Creative Commons Attribution (CC BY) license (<http://creativecommons.org/licenses/by/4.0/>).